

**New insight into the formation of  
hexamethylenetetramine (HMT) in interstellar and  
cometary ice analogs**

V Vinogradoff, F Duvernay, G Danger, P Theulé, T Chiavassa

► **To cite this version:**

V Vinogradoff, F Duvernay, G Danger, P Theulé, T Chiavassa. New insight into the formation of hexamethylenetetramine (HMT) in interstellar and cometary ice analogs. *Astronomy and Astrophysics* - A&A, EDP Sciences, 2011, 530, pp.A128. 10.1051/0004-6361/201116688 . hal-01076037

**HAL Id: hal-01076037**

**<https://hal.archives-ouvertes.fr/hal-01076037>**

Submitted on 20 Oct 2014

**HAL** is a multi-disciplinary open access archive for the deposit and dissemination of scientific research documents, whether they are published or not. The documents may come from teaching and research institutions in France or abroad, or from public or private research centers.

L'archive ouverte pluridisciplinaire **HAL**, est destinée au dépôt et à la diffusion de documents scientifiques de niveau recherche, publiés ou non, émanant des établissements d'enseignement et de recherche français ou étrangers, des laboratoires publics ou privés.

# New insight into the formation of hexamethylenetetramine (HMT) in interstellar and cometary ice analogs

V. Vinogradoff, F. Duvernay, G. Danger, P. Theulé, and T. Chiavassa

Université de Provence, Laboratoire de Physique des Interactions Ioniques et Moléculaires, Centre de St-Jérôme,  
Av Escadrille Normandie-Niemen, 13397 Marseille, France  
e-mail: [fabrice.duvernay@univ-provence.fr](mailto:fabrice.duvernay@univ-provence.fr)

Received 10 February 2011 / Accepted 5 April 2011

## ABSTRACT

**Aims.** We investigate the purely thermal formation of hexamethylenetetramine (HMT,  $C_6H_{12}N_4$ ) in interstellar ice analogs from non-photolysed ice and compare our results with those for the formation from photolysed ice.

**Methods.** We use Fourier transform-infrared spectroscopy to follow residue formation from VUV irradiation of  $H_2CO:NH_3$  ice mixture in different concentration ratios. We also report the warming of the  $H_2CO:NH_3:HCOOH$  ice mixture.

**Results.** We present the characterization of organic residues obtained at 330 K from VUV irradiation of  $H_2CO:NH_3$  ice mixtures. The organic residues contain compounds related to polyoxomethylene (POM,  $[-CH_2-O-]_n$ ) and HMT ( $C_6H_{12}N_4$ ). We report, for the first time, the formation of HMT from the warming of an interstellar ice analogs,  $H_2CO:NH_3:HCOOH$ , without any energetic processing (i.e. photons or particles). New insights into HMT formation mechanism are proposed. These results strengthen the hypothesis that HMT is present in interstellar grains or in comets, where it may be detected with the COSAC instrument of the Rosetta mission.

**Key words.** astrochemistry – ISM: molecules – methods: laboratory

## 1. Introduction

In molecular clouds, the chemical composition of the ice mantle on the interstellar grains evolves as clouds collapse to form protostars, and afterward main-sequence stars with planets and comets. As infrared absorption studies of protostellar environments have shown, many molecules are frozen into the ice mantle of dust grains (Whittet et al. 1996). The primitive ice composition can be processed by the protostar UV photons, cosmic rays, and ion bombardments. Newly formed molecules can eventually either be released into the gas phase or be incorporated into comets and planets (van Dishoeck et al. 1998). The nature of organic compounds within the icy mantle of interstellar grains or comets is crucial to understand the chemical evolution of materials from the interstellar medium to the solar system. A classical laboratory approach to understanding this chemical evolution is to start with various ice mixtures (ice analogs) at 10 K and photolyse them with vacuum ultraviolet (VUV) photons in order to simulate the energetic processing of dust ice mantle in molecular clouds. Once warmed to room temperature, these processed ice mixtures leave an organic residue (“yellow stuff”). This latter is presumed to be a close analog of dust organic mantles in molecular clouds (Allamandola et al. 1988; Briggs et al. 1992; Cottin et al. 1999). Among the complex organic refractory molecules that have been synthesized during cometary and interstellar ice analog experiments, polyoxymethylene (POM –  $(CH_2-O)_n$ ) and hexamethylenetetramine (HMT –  $C_6H_{12}N_4$ ) seem to be of prime interest. POM-like polymers have been detected when ice mixtures containing both formaldehyde and ammonia are slowly warmed up, without any photolysis or ion bombardment (Schutte et al. 1993). After VUV photolysis of mixtures such as  $H_2O:CH_3OH:CO:NH_3$ , POM-like polymers have also been detected, but in this case, HMT and HMT-derivatives are the main refractory products at 300 K (Bernstein et al. 1995; Muñoz Caro et al. 2003, 2004; Cottin et al. 2001). The suspected

pathway of HMT formation has been proposed on the basis of its synthesis in aqueous solution (Bernstein et al. 1995; Walker 1964). It appears from these previous studies that formaldehyde ( $H_2CO$ ), coming from  $CH_3OH$  photolysis, reacts thermally with  $NH_3$  to give after several steps HMT. One of these steps is the methylenimine ( $CH_2=NH$ ) formation. However, studies of a non-irradiated ice mixture containing  $H_2CO$  and  $NH_3$  in different ratios have shown that neither methylenimine nor HMT are observed in their conditions (Schutte et al. 1993; Bossa et al. 2009b). According to a theoretical work (Walch et al. 2001) dealing with the methylenimine formation from formaldehyde and ammonia an acid, playing the role of catalyst, should be needed to perform this reaction in ice.

We report on our study of the experimental photoprocessing and thermalprocessing of interstellar ice analogs, containing  $H_2CO$  and  $NH_3$  using IR spectroscopy to characterize the products in ice and refractory residue. These experiments show, for the first time a formation of HMT from purely thermal reaction (i.e. without any photons) of a  $H_2CO:NH_3$  ice mixture containing formic acid (HCOOH). All of these experiments were also performed in water dominated ices, in order to be closer to the interstellar ice composition where  $H_2O$  is the major constituent. The layout of this paper is as follows. In Sect. 2, we describe the experimental protocol. The experimental results are presented in Sect. 3, while the astrophysical implications are presented in Sect. 4.

## 2. Experimental

Ammonia ( $NH_3$ ) is commercially available as a 99.9995% pure gas from Air Liquide. Formaldehyde ( $H_2CO$ ) was bought under its paraformaldehyde polymer from Aldrich and was gently heated to be sublimated as a monomer. The  $H_2O:NH_3:H_2CO$  gas mixtures were prepared at room temperature into two primary vacuum pumped mixing lines, one for the  $H_2O:NH_3$  mixture

and one for H<sub>2</sub>CO, in order to prevent gas phase reactions from occurring. They were then co-deposited onto a copper surface cooled to 25 K by a ARS (Advanced Research Systems) cryo cold head within a high vacuum chamber (*c.a.* 10<sup>-8</sup> mbar). H<sub>2</sub>O:NH<sub>3</sub>:H<sub>2</sub>CO mixtures of different concentration ratios were deposited onto the cold surface. The IR spectra were recorded between 4000 and 650 cm<sup>-1</sup> in the reflexion mode using a Vertex 70 FTIR (Fourier Transform Infra-Red) spectrometer. A typical spectrum had a 1 cm<sup>-1</sup> resolution and was averaged over one hundred interferograms. The sample was warmed using a resistive heating wire and the temperature was controlled using a Lakeshore Model 331 temperature controller. The IR spectrum was monitored during the temperature ramp. The VUV radiation ( $\lambda > 120$  nm) was generated from a microwave discharge hydrogen flow lamp (Ophos instruments). The hydrogen lamp fluence was estimated to be *c.a.* 10<sup>15</sup> s<sup>-1</sup>cm<sup>-2</sup>. This fluence was used to determine the photo-dissociation cross-section of formaldehyde and ammonia. The concentration ratio of the different mixtures was first set before deposition using standard manometric techniques. It was then derived from the IR spectra by integrating the bands to estimate the column density of NH<sub>3</sub> and H<sub>2</sub>CO according to their band strengths following the equation  $N = \frac{\int \tau(\nu) d\nu}{A}$ , where  $N$  is the column density (Mol cm<sup>-2</sup>),  $\tau(\nu)$  the optical depth, and  $A$  the band strength (cm molecule<sup>-1</sup>). However, the ratio calculated depends on the band strengths provided by the literature. Moreover, the values of the band strengths depend on the nature, composition, and temperature of the ice in which molecules are found, and this dependence is a major source of uncertainty when evaluating the column densities of frozen molecules. For NH<sub>3</sub>, the band strengths of the wagging mode at 1070 cm<sup>-1</sup> varied from 1.3 × 10<sup>-17</sup> to 1.7 × 10<sup>-17</sup> cm molecule<sup>-1</sup> (Kerkhof et al. 1999; d’Hendecourt et al. 1986) in its pure solid form. We use the value given by Kerkhof et al. (1999): 1.3 × 10<sup>-17</sup> cm molecule<sup>-1</sup>, as usually done in the literature. For H<sub>2</sub>CO, we use the values given by Schutte et al. (1993): 9.6 × 10<sup>-18</sup> cm molecule<sup>-1</sup> for the CO stretch mode at 1725.5 cm<sup>-1</sup> and 3.9 × 10<sup>-18</sup> cm molecule<sup>-1</sup> for the CH<sub>2</sub> scissoring mode at 1494 cm<sup>-1</sup>. The thickness of the deposited solid films, assuming a density of 0.73 g cm<sup>-3</sup> and 0.92 g cm<sup>-3</sup> for NH<sub>3</sub> and H<sub>2</sub>O, respectively, was estimated to be around 0.1 μm, which is similar to the interstellar ice mantle thickness. We also used these band strengths to monitor the decrease in the NH<sub>3</sub> and H<sub>2</sub>CO IR bands intensities as they were consumed during the reaction and estimated how much of each of these products were formed.

### 3. Results

According to the mechanism proposed by Bernstein et al. (1995), H<sub>2</sub>CO and NH<sub>3</sub> are the key reactants to explain the formation of HMT, from an photolysed CH<sub>3</sub>OH:NH<sub>3</sub> ice mixture. We therefore study the photoprocessing of H<sub>2</sub>CO:NH<sub>3</sub> at 25 K and compare the residue composition obtained at 330 K with the one formed from the VUV photolysis of an ice mixture containing CH<sub>3</sub>OH and NH<sub>3</sub>.

#### 3.1. VUV irradiation of NH<sub>3</sub>:H<sub>2</sub>CO ice mixture at 25 K

Pure NH<sub>3</sub> and H<sub>2</sub>CO are co-deposited at 25 K within a 1:3 concentration ratio and the IR spectrum is displayed in Fig. 1. The assignment of each band is well known (Bossa et al. 2009b) and is reported in Table 1.

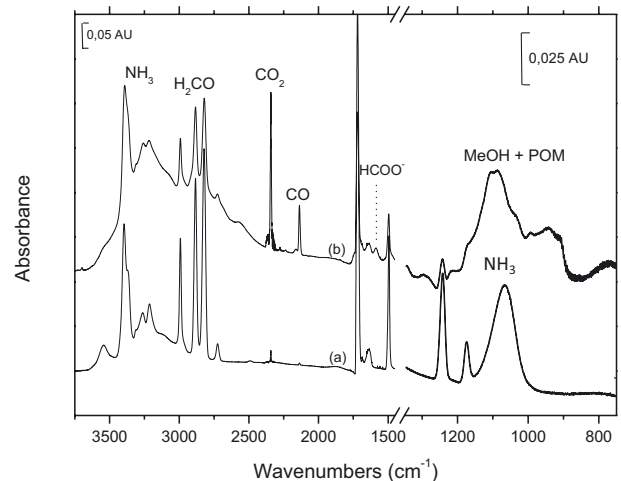


**Fig. 1.** Infrared spectra of (a) a NH<sub>3</sub>:H<sub>2</sub>CO binary mixture in a 1:3 concentration ratio at 25 K; (b) after a 4 h VUV irradiation of the same ice mixture at 25 K.

When the pure solid of H<sub>2</sub>CO is subjected to the 4 K min<sup>-1</sup> temperature ramp, it begins to sublime at 120 K in our vacuum chamber. On the basis of its IR signal, solid formaldehyde has fully disappeared at 135 K. Pure NH<sub>3</sub> begins to sublime at the same heating rate at 120 K and has fully disappeared at 125 K, in good agreement with a previous study (Sandford et al. 1993). We irradiate the NH<sub>3</sub>:H<sub>2</sub>CO ice mixture in a 1:3 concentration ratio at 25 K with VUV photons and follow its photolysis by IR spectroscopy as seen in Fig. 1. After 240 min of VUV irradiation, 62% of the amount of formaldehyde and 50% of the amount of NH<sub>3</sub> are consumed (Fig. 1). Their time decays are fitted with a first order kinetic rate. The corresponding kinetic constant are found to be 3.3 × 10<sup>-4</sup> s<sup>-1</sup> and 2.7 × 10<sup>-4</sup> s<sup>-1</sup> for formaldehyde and ammonia, respectively. With our photon fluence, the corresponding photodissociation cross-section can be estimated to be  $\sigma_{\text{photo}} = 3 \times 10^{-19}$  photon<sup>-1</sup> cm<sup>-2</sup> and  $\sigma_{\text{photo}} = 2.7 \times 10^{-19}$  photon<sup>-1</sup> cm<sup>-2</sup>. Those photodissociation cross-sections are in good agreement with a previous study reported by Cottin et al. (2003). In their study, the photo-dissociation cross-sections of ammonia vary from 2.7 × 10<sup>-19</sup> photon<sup>-1</sup> cm<sup>-2</sup> to 4.8 × 10<sup>-20</sup> photon<sup>-1</sup> cm<sup>-2</sup> as a function of the ice composition (Cottin et al. 2003). Besides the IR signatures of formaldehyde and ammonia, the irradiated sample displays the presence of new bands at 2341 and 2137 cm<sup>-1</sup> related to the formation of CO<sub>2</sub> and CO, respectively, as shown in Fig. 1. A clear band is also observed at 1585 cm<sup>-1</sup> that is related to the formation of HCOO<sup>-</sup> (Schutte et al. 1999). We also detected POM on the basis of its IR bands at 1109, and 944 cm<sup>-1</sup> overlapped by a broad band assigned to methanol at 1031 cm<sup>-1</sup>. Photochemistry of formaldehyde and ammonia are well known in both the gas and solid states (Cottin et al. 2003; Gerakines et al. 1996; Okabe 1978). The results of formaldehyde photolysis in the VUV region identify two primary means of forming radicals and molecules

$$\text{H}_2\text{CO} + h\nu \rightarrow \text{H}^\bullet + \text{HCO}^\bullet,$$

$$\text{H}_2\text{CO} + h\nu \rightarrow \text{H}_2 + \text{CO}.$$

For NH<sub>3</sub>, three main primary processes are found to occur in the near and vacuum ultraviolet photolysis

$$\text{NH}_3 + h\nu \rightarrow \text{NH}_2^\bullet + \text{H}^\bullet,$$

$$\text{NH}_3 + h\nu \rightarrow \text{NH} + \text{H}_2,$$

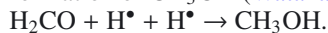
$$\text{NH}_3 + h\nu \rightarrow \text{NH} + \text{H}^\bullet + \text{H}^\bullet.$$

**Table 1.** Infrared spectra for H<sub>2</sub>CO/NH<sub>3</sub> 3:1 at 25K after 240 min of irradiation in our laboratory conditions.

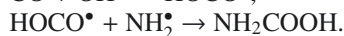
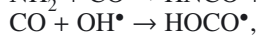
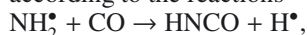
| Wavenumbers (cm <sup>-1</sup> ) | Assignment                      | molecules <sup>a</sup>                            | A (cm molec <sup>-1</sup> ) | Ref.                          |
|---------------------------------|---------------------------------|---|-----------------------------|-------------------------------|
| 3330-3010 b                     | $\nu(\text{OH})$                | <b>CH<sub>3</sub>OH</b>                           |                             |                               |
| 3393 s                          | $\nu(\text{NH})$                | <b>NH<sub>3</sub></b>                             |                             | (Kerkhof et al. 1999)         |
| 3256 m                          | $\nu(\text{NH})$                | <b>NH<sub>3</sub></b>                             |                             | (Kerkhof et al. 1999)         |
| 3215 m                          | $\nu(\text{NH})$                | <b>NH<sub>3</sub></b>                             |                             | (Kerkhof et al. 1999)         |
| 2992 s                          | $\nu(\text{CH})$                | <b>H<sub>2</sub>CO</b>                            |                             | (Schutte et al. 1993)         |
| 2883 s                          | $\nu(\text{CH})$                | <b>H<sub>2</sub>CO</b>                            |                             | (Schutte et al. 1993)         |
| 2819 s                          | $\nu(\text{CH})$                | <b>H<sub>2</sub>CO</b>                            |                             | (Schutte et al. 1993)         |
| 2726 m                          | $\nu(\text{CH})$                | <b>H<sub>2</sub>CO</b>                            |                             | (Schutte et al. 1993)         |
| 2341 vs                         | $\nu_{\text{as}}(\text{CO}_2)$  | <b>CO<sub>2</sub></b>                             | $7.6 \times 10^{-17}$       | (Gerakines et al. 1995)       |
| 2275 w                          | $\nu_{\text{as}}(\text{NCO})$   | <b>HOCN</b>                                       |                             |                               |
| 2234 vw                         | $\nu_{\text{as}}(\text{NCO})$   | <b>HNCO</b>                                       | $7.8 \times 10^{-17}$       | (van Broekhuizen et al. 2004) |
| 2161 w                          | $\nu_{\text{as}}(\text{NCO})$   | <b>OCN<sup>-</sup></b>                            |                             | (Raunier et al. 2003)         |
| 2137 m                          | $\nu(\text{CO})$                | <b>CO</b>   | $1.1 \times 10^{-17}$       | (Gerakines et al. 1996)       |
| 2089 vw                         | $\nu(\text{CN})$                | <b>HCN</b>  |                             |                               |
| 1722 s                          | $\nu(\text{C=O})$               | <b>H<sub>2</sub>CO</b>                            | $9.6 \times 10^{-18}$       | (Schutte et al. 1993)         |
| 1688 w                          | $\nu(\text{C=O})$               | <b>NH<sub>2</sub>COOH</b>                         | $5 \times 10^{-18}$         | (Bossa et al. 2008)           |
| 1638 w                          | $\delta\text{NH}$               | <b>NH<sub>3</sub></b>                             |                             | (Kerkhof et al. 1999)         |
| 1585 w                          | $\nu_{\text{as}}(\text{COO}^-)$ | <b>HCOO<sup>-</sup>NH<sub>4</sub><sup>+</sup></b> | $1 \times 10^{-16}$         | (Schutte et al. 1999)         |
| 1495 m                          | $\delta\text{CH}_2$             | <b>H<sub>2</sub>CO</b>                            | $3.9 \times 10^{-18}$       | (Schutte et al. 1993)         |
| 1389 vw                         | $\delta_{\text{s}}(\text{CH})$  | <b>HCOO<sup>-</sup>NH<sub>4</sub><sup>+</sup></b> | $1.7 \times 10^{-18}$       | (Schutte et al. 1999)         |
| 1348 vw                         | $\delta_{\text{as}}(\text{CH})$ |   |                             |                               |
| 1302 vw                         |                                 | <b>CH<sub>4</sub></b>                             | $3.8 \times 10^{-18}$       | (Hudgins et al. 1993)         |
| 1245 w                          | $\rho(\text{CH}_2)$             | <b>H<sub>2</sub>CO</b>                            |                             | (Schutte et al. 1993)         |
| 1168 w                          | $\nu(\text{CO})$                | <b>HCOOCH<sub>3</sub></b>                         |                             | (Gerakines et al. 1996)       |
| 1109 m                          |                                 | <b>POM</b>  |                             | (Schutte et al. 1993)         |
| 1070 m                          | $\omega(\text{NH})$             | <b>NH<sub>3</sub></b>                             | $1.3 \times 10^{-17}$       | (Kerkhof et al. 1999)         |
| 1031 w                          | $\nu(\text{CO})$                | <b>CH<sub>3</sub>OH</b>                           | $1.8 \times 10^{-17}$       | (Hudgins et al. 1993)         |
| 944 w                           | $\nu(\text{CO})$                | <b>POM</b>  | $3 \times 10^{-17}$         | (Schutte et al. 1993)         |
| 910 vw                          | $\nu(\text{CO})$                | <b>HCOOCH<sub>3</sub></b>                         |                             | (Gerakines et al. 1996)       |

**Notes.** Vibration mode: stretching ( $\nu$ ); bending ( $\delta$ ); rocking ( $\rho$ ); inversion ( $\omega$ ). as: asymmetric mode, s: symmetric mode. <sup>(a)</sup> Molecules in boldface are present before irradiation. Intensities: very strong (vs); strong (s); medium (m); weak (w); very weak (vw); and broad (b).

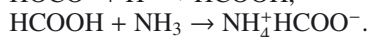
The hydrogenation processes within the ice can explain the formation of CH<sub>3</sub>OH (Watanabe et al. 2004)



It results from the presence of methanol in the mixture the formation, of methylformate HCOOCH<sub>3</sub> after VUV irradiation, as previously reported by Gerakines et al. (1996). CO is produced by the photo-dissociation of formaldehyde that leads to CO<sub>2</sub> formation by the reaction between an excited CO\* and CO (Okabe 1978). CO can also produce other molecules, such as carbamic acid NH<sub>2</sub>COOH (Bossa et al. 2008) and isocyanic acid HNCO according to the reactions



The acid-base reaction at low temperature between HCOOH and NH<sub>3</sub> is able to produce ammonium formate HCOO<sup>-</sup>NH<sub>4</sub><sup>+</sup> explaining the IR features located at 1585, and 1389 cm<sup>-1</sup> (Schutte et al. 1999)



The IR bands of products observed after irradiation at 25 K are reported in Table 1 and according to the ice composition, the amount of each of them is reported in Table 2. Unfortunately the total amount of some products cannot be estimated because of the overlapping of the IR features (e.g. methanol, carbamic acid).

In an ice-mixture where ammonia is in excess with respect to formaldehyde, after 4 h of irradiation at 25 K, we observe the same products as previously described for the NH<sub>3</sub>:H<sub>2</sub>CO 1:3 ice mixture. However their relative abundances differ between those

two experiments (Table 2). The amount of anionic species (i.e. OCN<sup>-</sup>, HCOO<sup>-</sup>) is more important with an excess of NH<sub>3</sub>. This can be explained by an acid-base reaction at 25 K involving isocyanic acid HNCO and formic acid HCOOH with residual NH<sub>3</sub>. In addition to an excess of NH<sub>3</sub>, in our experimental conditions, we cannot detect the POM because of the formaldehyde dilution within the ice.

The influence of water molecules on the ice composition observed after irradiation is also important because it is the main component in interstellar ices. In an H<sub>2</sub>O:H<sub>2</sub>CO:NH<sub>3</sub> ice mixture in a 10:1:3 concentration ratio, after irradiation at 25 K, the dominant products are CO<sub>2</sub> and HCOO<sup>-</sup>, which correspond to 18% and 16% of the products, respectively. Without water these species only represent 8% and 1.3% of the products respectively. The enhancement in the amount of CO<sub>2</sub> and HCOO<sup>-</sup> can be explained by the reaction between OH radical coming from water dissociation, with CO, leading to the formation of CO<sub>2</sub> but also formic acid HCOOH (Hudson et al. 1999), which in the presence of ammonia is quickly converted into ammonium formate.

### 3.2. Warming of NH<sub>3</sub>:H<sub>2</sub>CO photolysed ice

After the VUV irradiation of the NH<sub>3</sub>:H<sub>2</sub>CO ice mixture in a 1:3 concentration ratio, the sample was warmed to 330 K at a 4 K min<sup>-1</sup> rate (Fig. 2). The warming was monitored by IR spectroscopy. The spectrum and composition of the irradiated ice mixtures change greatly, while the temperature increases as seen in Fig. 2 and Table 2.

At 220 K, the infrared spectrum of the irradiated sample is dominated by new strong features in the NH stretching region at



**Table 2.** Ice composition after 4 h of VUV irradiation and warming at 330 K under our laboratory conditions.

|                                  | Species                           | $\text{H}_2\text{CO}/\text{NH}_3$<br>3/1 |                | $\text{H}_2\text{CO}/\text{NH}_3$<br>1/3 |                | $\text{H}_2\text{O}/\text{H}_2\text{CO}/\text{NH}_3$<br>10/1/3 |                | $\text{H}_2\text{O}/\text{H}_2\text{CO}/\text{NH}_3$<br>10/3/1 |                |
|----------------------------------|-----------------------------------|--|----------------|--|----------------|--|----------------|--|----------------|
|                                  |                                   | $N(\text{Mol cm}^{-2})$                  | % <sup>a</sup> | $N(\text{Mol cm}^{-2})$                  | % <sup>a</sup> | $N(\text{Mol cm}^{-2})$  | % <sup>a</sup> | $N(\text{Mol cm}^{-2})$  | % <sup>a</sup> |
| Initial                          | $\text{H}_2\text{CO}$             | $2.67 \times 10^{17}$                    |                | $7.52 \times 10^{16}$                    |                | $9.5 \times 10^{16}$   |                | $7.8 \times 10^{16}$   |                |
| After irradiation<br>4 h at 25 K | $\text{H}_2\text{CO}$             | $1 \times 10^{17}$                       |                | $1.87 \times 10^{16}$                    |                | $5.4 \times 10^{16}$   |                | $4.7 \times 10^{16}$   |                |
|                                  | $\text{CO}_2$                     | $8.84 \times 10^{15}$                    | 5              | $4.7 \times 10^{15}$                     | 8.4            | $7.4 \times 10^{15}$   | 18             | $3.7 \times 10^{14}$   | 12             |
|                                  | $\text{OCN}^-$                    | $1.7 \times 10^{14}$                     | 0.1            | $1.1 \times 10^{15}$                     | 2              | $1 \times 10^{15}$   | 2.5            | $1.9 \times 10^{14}$   | 0.6            |
|                                  | $\text{HNCO}$                     | $7.95 \times 10^{13}$                    | 0.05           |  |                |  |                |  |                |
|                                  | $\text{HCOO}^-$                   | $1.05 \times 10^{15}$                    | 0.6            | $7.5 \times 10^{14}$                     | 1.3            | $6.4 \times 10^{15}$   | 16             | $3.2 \times 10^{14}$   | 1              |
|                                  | $\text{CO}$                       | $2.92 \times 10^{16}$                    | 17             | $4.14 \times 10^{15}$                    | 7.3            | $6.3 \times 10^{15}$   | 15             | $3.9 \times 10^{15}$   | 12.4           |
|                                  | $\text{POM}$                      | $1.24 \times 10^{16}$                    | 7.4            |  |                |  |                |  |                |
| At 220 K                         | $\text{NH}_2\text{CH}_2\text{OH}$ | $2.5 \times 10^{16}$                     | 9.4            | $6.93 \times 10^{15}$                    | 12.2           | $1.03 \times 10^{15}$  | 2.5            | $1.4 \times 10^{15}$   | 4.5            |
|                                  | $\text{OCN}^-$                    |  |                | $3.85 \times 10^{14}$                    | 0.7            | $2 \times 10^{14}$   | 0.5            | $3.9 \times 10^{13}$   | 0.12           |
|                                  | $\text{HCOO}^-$                   | $6.7 \times 10^{15}$                     | 2.5            | $1.9 \times 10^{14}$                     | 0.34           | $1.6 \times 10^{14}$   | 0.4            | $5 \times 10^{13}$   | 0.16           |
|                                  | $\text{NH}_2\text{COOH}$          | $5.3 \times 10^{16}$                     | 20             |  |                |  |                |  |                |
|                                  | $\text{NH}_2\text{COH}$           | $2.7 \times 10^{15}$                     | 1              |  |                |  |                |  |                |
|                                  | $\text{POM}$                      | $6 \times 10^{16}$                       | 22             |  |                |  |                | $1.8 \times 10^{15}$   | 6              |
| Residue at 330 K                 | $\text{POM}$                      | $9.2 \times 10^{14}$                     | 0.4            |  |                |  |                | $1.8 \times 10^{14}$   | 0.6            |
|                                  | $\text{HMT}$                      |  |                | $3.5 \times 10^{14}$                     | 0.6            | $6 \times 10^{14}$   | 1.5            |  |                |

**Notes.** <sup>(a)</sup> The yields (in %) after irradiation at 25 K are calculated using the amount of formaldehyde that has been photolysed, while the yields of products (in %) observed during the warming up are calculated using the initial amount of formaldehyde.

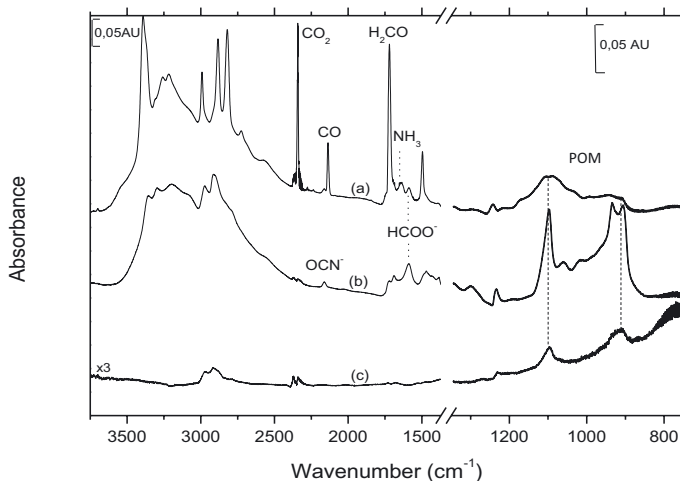


**Fig. 2.** Infrared spectrum (a) of a  $\text{NH}_3:\text{H}_2\text{CO}$  binary mixture in a 1:3 concentration ratio after 4 h of VUV irradiation at 25 K, and subsequent warming at (b) 220 K, (c) 330 K

3342, 3292  $\text{cm}^{-1}$ , in the CH region at 2967, 2906  $\text{cm}^{-1}$ , and also in the C-O/C-N region at 1095 and 921  $\text{cm}^{-1}$ . These changes during the warming can be understood as thermal reactions occurring between species observed at 25 K after the VUV irradiation. The thermal reactions in ice are known to follow the Arrhenius law (Bossa et al. 2009b,a; Duvernay et al. 2010), so increasing the temperature, increases the reaction rate, and also the diffusion of species within the ice. This latter point is especially true for barrier-less reactions such as radical-radical reactions. In addition, the most volatile compounds ( $\text{CO}$ ,  $\text{CO}_2$ ,...) have been desorbed, and are no longer present at 220 K in our laboratory conditions. The strong NH bands are assigned to the aminomethanol ( $\text{NH}_2\text{CH}_2\text{OH}$ ) formed by the thermal reaction between  $\text{NH}_3$  and  $\text{H}_2\text{CO}$  (Bossa et al. 2009b). The strong bands located at 1100 and 930  $\text{cm}^{-1}$  are easily assigned to

the POM-like species thermally produced from the  $\text{NH}_3$  catalyzed formaldehyde polymerization (Schutte et al. 1993). The branching ratio of  $\text{NH}_2\text{CH}_2\text{OH}$  to POM depends on the concentration ratio of ammonia to formaldehyde. It has been shown by Schutte et al. (1993) and Bossa et al. (2009b) that when  $[\text{H}_2\text{CO}]/[\text{NH}_3] > 1$ , the POM molecules are the dominant products, while when the ratio is lower than 1, the aminomethanol is the dominant product. In water-dominated ice, aminomethanol is the main product observed at 220 K (Bossa et al. 2009b) (see Table 2). Finally, the column density of the species observed at 220 K is derived using the band strengths of each product and is in Table 2. In addition of POM and aminomethanol, some other products are also observed such as carbamic acid ( $\text{NH}_2\text{COOH}$ ), ammonium formate ( $\text{HCOO}^-\text{NH}_4^+$ ), and formamide ( $\text{NH}_2\text{CHO}$ ).

After these samples were warmed to 330 K, the absorbance on the IR spectrum is typically 5 times weaker than the one observed in the samples at 220 K, indicating that a considerable amount of material is lost by desorption between 220 and 330 K (Fig. 2). The organic film that remains on the substrate at 330 K is therefore composed of refractory compounds. The nature of this residue depend on the composition of the initial ice (Tables 2 and 3, Fig. 3). When the  $[\text{H}_2\text{CO}]/[\text{NH}_3]$  ratio is greater than 1 (in the presence of or without water), the residue obtained after 4 h of VUV irradiation, followed by the warming of the ice at 330 K, is dominated by the POM molecule. When this ratio is smaller than 1, in the same conditions of fluence and temperature, the residue is dominated by the HMT molecule (Fig. 3, Tables 2 and 3). If we substitute  $\text{H}_2\text{CO}$  with  $\text{CH}_3\text{OH}$  in the mixture, we do not observe HMT after photolysis (4 h) and warming at 330 K. However, an extended VUV irradiation (12 h) of  $\text{CH}_3\text{OH}:\text{NH}_3$  ice-mixtures is known to produce HMT (Bernstein et al. 1995; Muñoz Caro et al. 2003; Cottin et al. 2001) because  $\text{H}_2\text{CO}$  is produced in larger amounts (Table 3). Therefore,  $\text{H}_2\text{CO}$  is a more effective precursor of HMT than  $\text{CH}_3\text{OH}$ , this result being consistent with Bernstein's mechanism. This mechanism, which is based on HMT synthesis in aqueous solution, involves

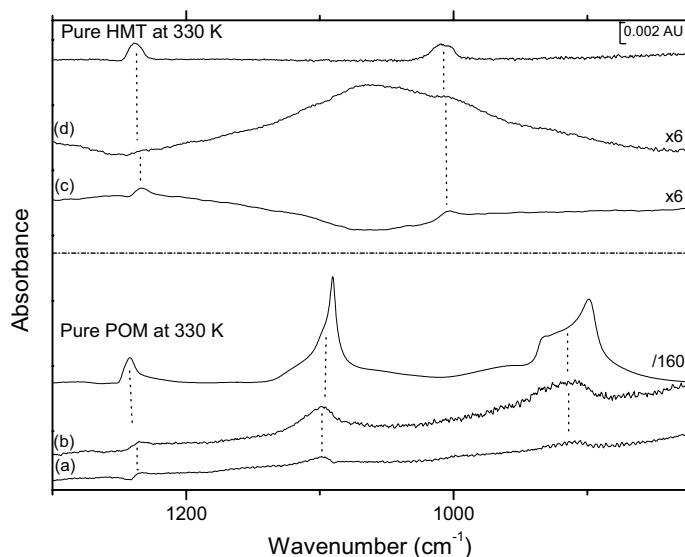


**Fig. 3.** Comparison between IR spectra of pure POM and HMT at 330 K with IR spectra of residue at 330 K obtained after 4 h of VUV irradiation for different initial ice composition (a) H<sub>2</sub>O:H<sub>2</sub>CO:NH<sub>3</sub> mixture in a 10:3:1 concentration ratio, (b) H<sub>2</sub>CO:NH<sub>3</sub> mixture in a 3:1 concentration ratio, (c) H<sub>2</sub>O:H<sub>2</sub>CO:NH<sub>3</sub> mixture in a 10:1:3 concentration ratio, (d) H<sub>2</sub>CO:NH<sub>3</sub> mixture in a 1:3 concentration ratio.

**Table 3.** Major compounds observed in the residue as a function of initial ice composition and VUV dose.

| Ice composition  | VUV dose(h) | Residue(330 K)   |
|--|-------------|------------------|
| H <sub>2</sub> CO:NH <sub>3</sub> 1:3                              | 4           | HMT              |
| H <sub>2</sub> CO:NH <sub>3</sub> 3:1                              | 4           | POM              |
| H <sub>2</sub> O:H <sub>2</sub> CO:NH <sub>3</sub> 10:1:3          | 4           | HMT              |
| H <sub>2</sub> O:H <sub>2</sub> CO:NH <sub>3</sub> 10:3:1          | 4           | POM              |
| H <sub>2</sub> O:CH <sub>3</sub> OH:NH <sub>3</sub> 20:1:1         | 4           | –                |
| H <sub>2</sub> O:CH <sub>3</sub> OH:NH <sub>3</sub> 20:1:1         | 12          | HMT <sup>a</sup> |
| H <sub>2</sub> CO:NH <sub>3</sub> 1:3                              | 0           | –                |
| H <sub>2</sub> CO:NH <sub>3</sub> 3:1                              | 0           | POM              |
| H <sub>2</sub> CO:NH <sub>3</sub> :HCOOH 1:6:1                     | 0           | HMT              |
| H <sub>2</sub> O:H <sub>2</sub> CO:NH <sub>3</sub> :HCOOH 10:1:6:1 | 0           | HMT              |

Notes. <sup>(a)</sup> Muñoz Caro et al. (2003).

several steps (Bernstein et al. 1995). The first is the photochemical conversion of CH<sub>3</sub>OH to H<sub>2</sub>CO. The second step is the formation from H<sub>2</sub>CO and NH<sub>3</sub> of methylenimine (CH<sub>2</sub>NH), which is the intermediate product in HMT formation. This step involves an activation barrier that needs to be overcome to form methylenimine. Hence, it is possible that the methylenimine production can be induced by an appropriate intermediate species (Bernstein et al. 1995). In the absence of this intermediate product, the thermal reaction between H<sub>2</sub>CO and NH<sub>3</sub> leads to the formation of aminomethanol (Bossa et al. 2009b). A theoretical approach has shown that the dehydration reaction of aminomethanol leading to the formation of methylenimine is possible in ice only if the reaction is catalyzed by an acid (Walch et al. 2001). The proposed mechanism is:

AH + B → A<sup>-</sup> BH<sup>+</sup> acid-base reaction;

H<sub>2</sub>CO + NH<sub>3</sub> + BH<sup>+</sup> → H<sub>2</sub>NCH<sub>2</sub>OH<sub>2</sub><sup>+</sup> + B aminoethanol formation;

H<sub>2</sub>NCH<sub>2</sub>OH<sub>2</sub><sup>+</sup> + A<sup>-</sup> → CH<sub>2</sub>NH + H<sub>2</sub>O + AH aminomethanol dehydration.

Moreover this acidic species has to be a common product in methanol and formaldehyde photolysed ice. From previous studies and our results, it seems that this acid, AH in the previous mechanism, could be formic acid HCOOH.

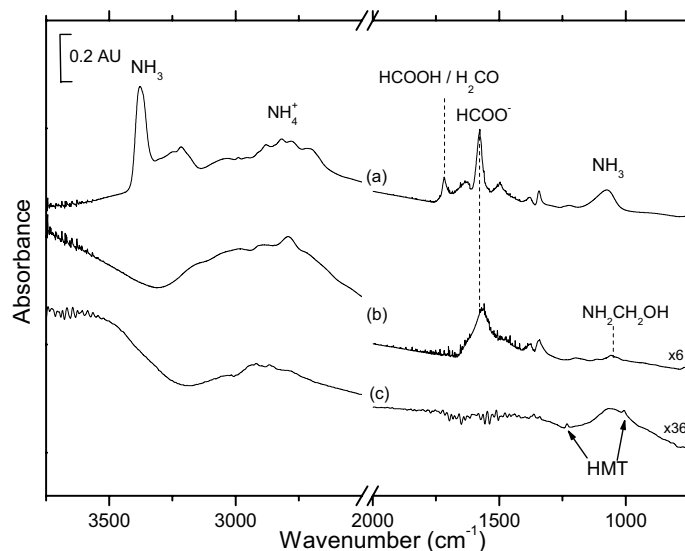


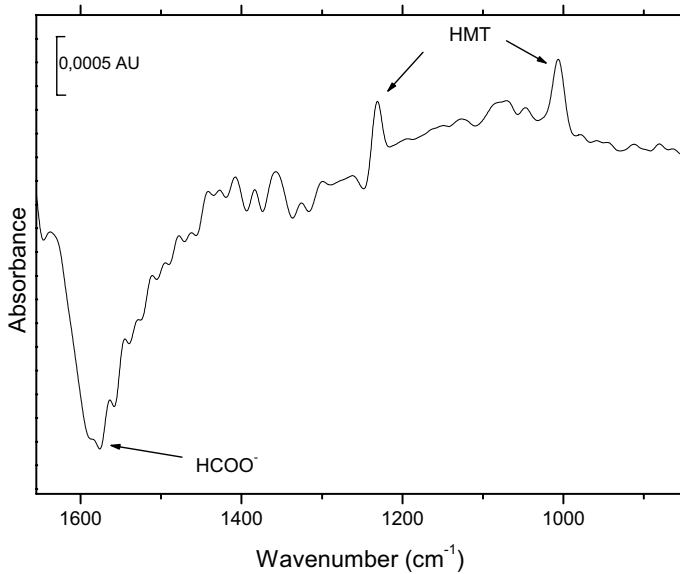
**Fig. 4.** FTIR spectrum of H<sub>2</sub>CO:NH<sub>3</sub>:HCOOH ice mixture in a 1:6:1 concentration ratio at (a) 15 K, (b) 220 K, (c) 330 K.

In the next section, we propose to verify this mechanism by studying the thermal reaction between H<sub>2</sub>CO, NH<sub>3</sub>, and HCOOH.

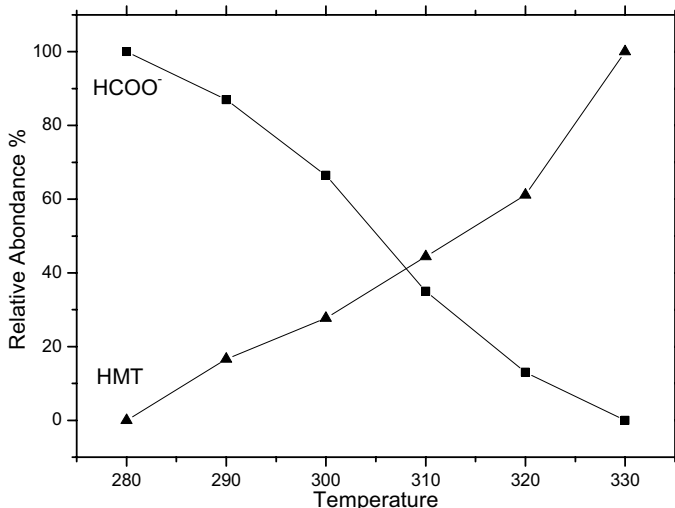
### 3.3. Thermal formation of HMT

Figure 4 shows the thermal evolution of a H<sub>2</sub>CO:NH<sub>3</sub>:HCOOH ice mixture in a 1:6:1 concentration ratio from 15 K to 330 K. At 15 K, the IR spectrum was dominated by a strong feature at 1585 cm<sup>-1</sup> assigned to HCOO<sup>-</sup>. Indeed, the ammonium formate HCOO<sup>-</sup>NH<sub>4</sub><sup>+</sup> is formed at low temperature ( $T < 40$  K) from HCOOH and NH<sub>3</sub> (Schutte et al. 1999). After the disappearance of the reactants, at 220 K the IR spectrum represents the addition of the IR spectra of ammonium formate and aminomethanol. At 330 K, the organic residue is easily assigned to HMT from its IR bands located at 1007 cm<sup>-1</sup> and 1235 cm<sup>-1</sup> (Fig. 4). Here the HMT is formed without any photons, just by thermal activation. It is important to note that if HCOOH is not present in the ice-mixture, no HMT is observed (Schutte et al. 1993; Bossa et al. 2009b) but only aminomethanol. From the IR spectrum, it is difficult to define at which temperature HMT was formed because of spectral confusion with NH<sub>3</sub> and aminomethanol bands. On the basis of the IR spectrum, HMT does not seem to have formed immediately when room temperature was reached. At 300 K, only the HCOO<sup>-</sup> feature was observed at 1585 cm<sup>-1</sup>. The HMT features were gradually formed as the temperature increases from 300 to 330 K while in the meantime, the feature located at 1585 cm<sup>-1</sup> decreases (see Fig. 5). Consequently, HMT seems to have formed only at the final stage of the experiment (i.e. 300–330 K). This result has been already observed in this work during the warming of a photolysed-ice with formaldehyde and ammonia (see Sect. 3.2), but also during the warming of a photolysed-ice with methanol and ammonia (Muñoz Caro et al. 2003). In the latter study, the authors suggest that the feature around 1585 cm<sup>-1</sup> could be assigned to carboxylic acid salts RCOO<sup>-</sup>NH<sub>4</sub><sup>+</sup>. According to them, this salt is crucial for the formation of HMT.

In our experiment, the feature located around 1585 cm<sup>-1</sup> can only be the formate ion HCOO<sup>-</sup>. This latter ion could be associated with NH<sub>4</sub><sup>+</sup>. Unfortunately, the ammonium formate is known to sublime around 230 K in laboratory conditions. Hence,



**Fig. 5.** FTIR difference between the spectra of  $\text{H}_2\text{CO}:\text{NH}_3:\text{HCOOH}$  ice mixture in a 1:6:1 concentration ratio at 330 K and 300 K.



**Fig. 6.** Thermal evolution of the relative abundances of  $\text{HCOO}^-$  and HMT between 280 and 330 K.

the counter ion of  $\text{HCOO}^-$  at 300 K cannot be the ammonium  $\text{NH}_4^+$ . As shown in Fig. 6, HMT features are gradually formed while the feature of  $\text{HCOO}^-$  decreases (Fig. 6). Because their evolutions are correlated, the counter ion of  $\text{HCOO}^-$  at 300 K seems to be the HMT cation. Indeed HMT could be formed at lower temperature, and because it is a base similar to  $\text{NH}_3$ , it could react with  $\text{HCOOH}$  giving a salt  $[\text{HCOO}^-][\text{C}_6\text{H}_{12}\text{N}_4\text{H}^+]$  (Blazevic et al. 1979). At temperatures higher than 300 K, the reverse acid-base reaction release the HMT and  $\text{HCOOH}$ . HMT remains on the substrate, while  $\text{HCOOH}$  sublimates. This experiment was also performed with an excess of water in order to form HMT in interstellar conditions. The thermal evolution of a  $\text{H}_2\text{O}:\text{H}_2\text{CO}:\text{NH}_3:\text{HCOOH}$  ice mixture in a 10:1:6:1 concentration ratio from 15 K to 330 K, leads to the formation of HMT but in a smaller proportion (Table 3). In this case,  $\text{H}_2\text{O}$  molecules do not promote the reaction but instead separate the reactants, making the formation of aminomethanol more difficult. However,  $\text{H}_2\text{O}$  is known to sublime around 180 K in laboratory conditions, while at 200 K both features of aminomethanol and  $\text{HCOO}^-$  are still observed. In these conditions, the step of

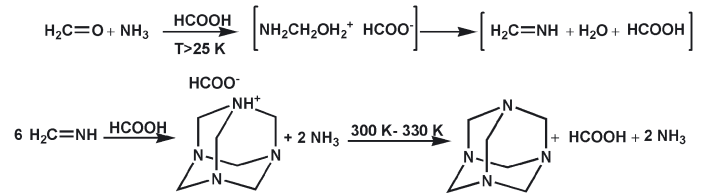


**Fig. 7.** Suspected chemical pathway for the formation of HMT. Species between brackets are not seen in our experiments and are possible intermediate species.

aminomethanol dehydration is unaffected by water in the HMT formation.

According to these results, we can propose a new insight on the HMT formation in interstellar ice analogs. Bernstein et al. (1995) state that the HMT production implies that the key chemical reaction steps involve an activation barrier that UV photons can help to overcome. According to these authors, the available thermal energy may be insufficient to surmount this barrier and the methylenimine production is induced by the photofragment of either  $\text{H}_2\text{CO}$  or  $\text{NH}_3$ , which produces an appropriate intermediate species that drives methylenimine production. From our results, it appears that HMT formation is not activated by UV photons but that the thermal available energy is sufficient, in the presence of an acid, to activate the HMT formation. In the presence of acids, the aminomethanol, produced by the thermal reaction between  $\text{H}_2\text{CO}$  and  $\text{NH}_3$ , can spontaneously dehydrate forming the methylenimine ( $\text{CH}_2=\text{NH}$ ), as also supported by a theoretical study (Walch et al. 2001). As previously proposed, the additional polymerization of methylenimine leads to the formation of HMT (Bernstein et al. 1995; Braillon et al. 1982), which is stored as a salt for temperatures lower than 300 K and in its neutral form above 300 K because of the salt decomposition (Fig. 7).

#### 4. Discussion and astrophysical implications

Planetary systems are formed from dust grains and gas in star-forming regions. The solid material in planetary systems, such as comets, asteroids, and planets, originates in primordial interstellar dust agglomerations and gas accretion. Complex organic molecules are present in a large variety of environments in space. For example, carbonaceous chondrites contain both carboxylic and amino acids (Cronin & Pizzarello 1997, 1999). Therefore, comets and asteroids likely provide a reservoir of molecules that can be considered as a prebiotic precursor on the early Earth through the cometary-bombardment. Among these complex organic molecules, HMT and POM-like, molecules are of prime interest as they are widely produced from photolysed-warmed interstellar ice analogs, containing methanol and ammonia, two interstellar molecules that have already been detected in interstellar grains (Boogert et al. 2008). Furthermore, from an astrobiological point of view, HMT is an interesting molecule that provide amino acids in acidic-solution (Wolman et al. 1971).

So far, there has not yet been any direct observation of those two molecules in either the solid phase (comets, grains) or gas phase. Bernstein et al. (1995) suggested that the degradation of HMT on cometary grains ejected from the nucleus could possibly be responsible for the extended source of the CN radical observed in comet Halley (Cottin et al. 2001). This could be an interesting indirect detection of HMT, but remains disputed (Cottin et al. 2001). The lack of solid phase detection of HMT

could be due, as shown in this work, to its very weak IR absorption when it is stored as salt in ice.

POM is suspected to be responsible for the extended source of formaldehyde (Huebner et al. 1987; Fray et al. 2006). It has been proposed that gaseous H<sub>2</sub>CO could be released by the thermal and photochemical degradation of polyoxymethylene that might be present in grains. The coming in situ investigation of cometary nucleus with the Rosetta mission would be able to search for those two molecules using the COSAC instrument (GC-MS) for HMT and the COSIMA instrument (secondary ion mass spectrometer) for POM-like molecules.

The POM formation mechanism in interstellar ice analogs is well known. POM and polymers of the same family have been detected when ice mixtures containing formaldehyde and ammonia are slowly warmed to room temperature, without any photolysis or ion bombardment (Schutte et al. 1993). Hence, it is often suggested that POM-like molecules are good indicators of the thermal processing of ice (Cottin et al. 2001), while, according to Bernstein's mechanism, HMT is a reliable indicator of VUV photolysis. Those two hypotheses may represent too tight constraints as POM has already been formed during photolysis and warming of interstellar ice analogs (this work, Bernstein et al. 1995), while HMT, in this work, is produced during the warming of an interstellar ice analogs H<sub>2</sub>CO:NH<sub>3</sub>:HCOOH:H<sub>2</sub> without any energetic processing (i.e. photons or particles). H<sub>2</sub>CO, NH<sub>3</sub>, and HCOOH have been detected in interstellar ices (Boogert et al. 2008) and can be formed within the ice without VUV photons. Formaldehyde is likely to be formed on ice by means of the hydrogenation of CO (Watanabe et al. 2004). HCOOH can be formed for example by proton bombardment of a CO:H<sub>2</sub>O ice mixture (Hudson et al. 1999). As thermal, photon, and cosmic-ray processes are important at one time or another in a comet's history, the detection of HMT or/and POM-like molecules in cometary nuclei would not help us to deduce the details of cometary chemical history as previously supposed (Bernstein et al. 1995; Cottin et al. 2001). A clearer understanding of all the processes that can happen within the ice coupled with a cometary model, would help us to significantly improve our understanding of comet composition and history.

## 5. Conclusion

Our experiments have shown that solid phase photolysis at 25 K of H<sub>2</sub>CO:NH<sub>3</sub> ice mixtures generates efficiently organic residue at room temperature. The nature of the residue depends on the initial ice composition. If formaldehyde is in excess with respect to ammonia, the POM is the main residue, while when ammonia is in excess with respect to formaldehyde, HMT is the main product. Comparison with previous studies have been made and demonstrate that formaldehyde ice is a more likely precursors to HMT production than methanol ice. We also demonstrate for the

first time that HMT can be formed thermally in interstellar ice analogs H<sub>2</sub>CO:NH<sub>3</sub>:HCOOH, without any energetic processing (photons or particles). HCOOH is primordial for HMT formation as it catalyzes the formation of methylenimine (CH<sub>2</sub>=NH) by means of aminomethanol (NH<sub>2</sub>CH<sub>2</sub>OH) dehydration. Hence, HMT can no longer be considered as a reliable indicator of VUV photolysis of ice.

*Acknowledgements.* This work has been funded by the French national program Physique Chimie du Milieu Interstellaire (PCMI) and the Centre National des Etudes Spatiales (CNES).

## References

- Allamandola, L. J., Sandford, S. A., & Valero, G. J. 1988, *Icarus*, 76, 225  
 Blazevic, N., Kolbah, D., Belin, B., Sunjic, V., & Kajfez, F. 1979, *Synthesis*, 3, 161  
 Braillon, B., Lasne, M., Ripoll, J., & Denis, J. 1982, *Nouv. J. Chim.*, 6, 121  
 Bernstein, M. P., Sandford, S. A., Allamandola, L. J., Chang, S., & Scharberg, M. A. 1995, *ApJ*, 454, 327  
 Bossa, J., Theule, P., Duvernay, F., Borget, F., & Chiavassa, T. 2008, *A&A*, 492, 719  
 Bossa, J., Duvernay, F., Theule, P., Borget, F., et al. 2009a, *A&A*, 506, 601  
 Bossa, J., Theule, P., Duvernay, F., & Chiavassa, T. 2009b, *ApJ*, 707, 1524  
 Boogert, A. C. A., Pontoppidam, K. M., Knez, C., et al. 2008, *ApJ*, 678, 985  
 Briggs, R., Ertem, G., Ferris, J. P., et al. 1992, *Orig. Life Evol. Biosph.*, 22, 287  
 Cottin, H., Gazeau, M. C., & Raulin, F. 1999, *Planet. Space Sci.*, 47, 1141  
 Cottin, H., Spzopa, C., & Moore, M. 2001, *ApJ*, 561, L139  
 Cottin, H., Morre, M., & Benilan, Y. 2003, *ApJ*, 590, 874  
 Cronin, J. R., & Pizzarello, S. 1997, *Science*, 275, 951  
 Cronin, J. R., & Pizzarello, S. 1999, *Adv. Space Res.*, 23, 293  
 D'Hendecourt, L. B., & Allamandola, L. J. 1986, *A&ASS*, 64, 453  
 Duvernay, F., Dufaure, V., Danger, G., et al. 2010, *A&A*, 523, A79  
 Fray, N., Benilan, Y., Biver, N., et al. 2006, *Icarus*, 184, 239  
 Gerakines, P. A., Schutte, W. A., Greenberg, J. M., & Vandishoeck, E. F. 1995, *A&A*, 296, 810  
 Gerakines, P. A., Schutte, W. A., & Ehrenfreund, P. 1996, *A&A*, 312, 289  
 Hudgins, D., Sandford, S., Allamandola, L., & Tielens, A. 1993, *ApJS*, 86, 713  
 Hudson, R. L., & Moore, M. H. 1999, *Icarus*, 140, 451  
 Huebner, W., Boice, D., & Sharp, C. 1987, *ApJ*, 320, L149  
 Kerkhof, O., Schutte, W., & Ehrenfreund, P. 1999, *A&A*, 346, 990  
 Muñoz Caro, G. M., & Schutte, W. A. 2003, *A&A*, 412, 121  
 Muñoz Caro, G. M., Meierhenrich, U., Schutte, W. A., Thiemann, W., & Greenberg, J. M. 2004, *A&A*, 413, 209  
 Okabe, H. 1978, *Photochemistry of Small Molecules* (New York: John Wiley & Sons, Inc), 269  
 Raunier, S., Chiavassa, T., Marinelli, F., Allouche, A., & Aycard, J. 2003, *Chem. Phys. Lett.*, 368, 594  
 Sandford, S. A., & Allamandola, L. J. *ApJ*, 1993, 417, 815  
 Schutte, W. A., Allamandola, L. J., & Sandford, S. A. *Icarus* 1993, 104, 118  
 Schutte, W., Boogert, A., Tielens, A., et al. 1999, *A&A*, 343, 966  
 Walker, J. F. 1964, *Formaldehyde* (New York: Reinhold Publishing Co.), 511  
 van Broekhuizen, F., Keane, J., & Schutte, W. *A&A*, 2004, 415, 425  
 van Dishoeck, E., & Blake, G. 1998, *ARA&A*, 36, 317  
 Walch, S., Bauschlicher, C., Ricca, A., & Bakes, E. 2001, *Chem. Phys. Lett.*, 333, 6  
 Watanabe, N., Nagaoka, A., Shiraki, T., & Kouchi, A. 2004, *ApJ*, 616, 638  
 Whittet, D., Schutte, W., Tielens, A., et al. 1996, *A&A*, 315, L357  
 Wolman, Y., Miller, S., Ibañez, J., & Oro, J. 1971, *Science*, 174, 1039